ELSEVIER

Journal of Alloys and Compounds 224 (1995) 22–28

Journal of ALLOYS AND COMPOUNDS

Characterization of the nitridation process of boric acid

X. Gouin [a,*], P. Grange [a], L. Bois [b], P. L'Haridon [b], Y. Laurent [b]

[a] *Unité de Catalyse et Chimie des Matériaux Divisés, Université Catholique de Louvain, Place Croix du Sud, 2, Boîte 17, 1348 Louvain-la-Neuve, Belgium*

[b] *Laboratoire de Chimie des Matériaux, URA 1496 CNRS, "Verres et Céramiques", Université de Rennes I, Campus de Beaulieu, av. du Gen. Leclerc, 35042 Rennes, France*

Received 28 December 19 94

Abstract

Boric acid $B(OH)_3$ has been thermally nitrided under flowing ammonia into a boron oxynitride. This reaction has been followed using various structural techniques: X-ray photoelectron spectroscopy (XPS), infrared spectroscopy (IR), X-ray diffraction and chemical analyses. Reaction of boric acid with ammonia began at 155 °C. The weight percent of nitrogen increases with the temperature of the pyrolysis process. Formation of B–N bonds is observed at 400 °C by infrared spectroscopy. Two boron species are observed by XPS and identified as boron linked mostly to oxygen atoms and as boron linked mostly to nitrogen atoms, denoted BO_x and BN_x, respectively. The intensity of the BN_x signal increases with the pyrolysis temperature.

Keywords: Boron oxynitride; XPS characterization; Boric acid; Nitridation

1. Introduction

An important non-oxide ceramic is boron nitride. Hexagonal boron nitride has a layered, graphite-like structure, consisting of B_3N_3 hexagons. B and N atoms alternate along the z direction. Boron nitride possesses chemical stability, electrical resistivity and high thermal conductivity. It is a material of great interest in the industrial field [1–4]. Nevertheless, powder synthesis using traditional high temperature methods do not allow easy shaping and the new interest in boron nitride is due to the development of new ways of synthesis, such as CVD [5–9] and polymeric routes [3,10–15]. Our interest is not in the synthesis of boron nitride but to get a better understanding of the chemical evolution occurring during the formation of boron nitride by boric acid nitridation, which is one of the traditional methods of synthesizing boron nitride [1,16–18]. It is already known that disordered boron nitride is obtained at 900 °C and that hot pressing at 1800 °C is used to get the crystallized hexagonal form [1,18,19]. These are called turbostratic boron nitride in accordance with the disordered forms of graphitic carbon [2]. The hexagonal layers are randomly stacked. The objective of the present paper was to follow the chemical evolution of boric acid under flowing ammonia at high temperatures up to 1300 °C. The nitridation process has been followed by X-ray photoelectron analysis (XPS), infrared spectroscopy (IR), X-ray diffraction (XRD) and chemical analyses.

2. Experimental section

2.1. Sample preparation

The boron oxynitride powders were prepared by the reaction of gaseous ammonia with boric acid at increasing temperatures. Commercial boric acid $B(OH)_3$, with low specific surface area, was used. In order to avoid melting which occurs at 169 °C, in a first step, boric acid was heated in a tubular furnace under flowing ammonia (40 l h^{-1}) at 155 °C. The heating rate was 3 °C min^{-1} and the maximum temperature was maintained for 3 h. Cooling was performed under flowing nitrogen. This first reaction provides partially nitrided white powders ready for further thermal treatments. The powders were then nitrided at the same conditions at higher temperatures: 400 °C, 600 °C, 1000 °C and 1300 °C. The 1300 °C sample was prepared in a furnace with no controlled heating rate. Furthermore, a commercial boron nitride powder was chosen as a reference compound.

* Corresponding author.

SSDI 0925-8388(95)01532-9

2.2. Characterization

Elemental analysis of oxygen and nitrogen were performed using Leco equipment (analyzer TC 436 and furnace EF400). Calibration was performed with CO_2 and N_2 gases.

X-ray diffraction spectra were recorded using a PW 3710 mdp control Philips generator equipped with an X-PERT goniometer system. A step size of 0.05° and a time per step of 1 s were used.

Infrared spectra were recorded with Bonem equipment (Michelson 100) from 400 cm^{-1} to 4000 cm^{-1} using KBr pellets.

The elemental surface composition of the samples was determined by X-ray photoelectron spectroscopy (XPS). The XPS analyses were performed on a SSX Model 206 spectrometer (Surface Science Instrument) equipped with a monochromatic Al Kα X-ray source (1486.6 eV). The effect of sample charging was compensated by an electron flood gun set at 6 eV, with a nickel grid placed 3 mm above the sample surface. A base pressure of 10^{-8} Pa was maintained during the analyses. High resolution B 1s, O 1s, N 1s and C 1s spectra were obtained by scanning the appropriate 10 eV energy windows while using an analyzer pass energy of 50 eV. The unresolved XPS peaks were decomposed into subcomponents using a Gaussian (85%)–Lorentzian (15%) curve fitting program with a non-linear background. The quantitative analyses were performed with the sensibility factors given by Scofield [20]. The binding energies reported in this work were referenced to the C 1s line at 284.8 eV. The carbon was present on every sample as residual hydrocarbon contaminant.

3. Results and discussion

3.1. Chemical analysis

Chemical analysis data are reported in Fig. 1 and Table 1. It can be noted that chemical analysis seems to be inconsistent, since the sum is often below 100%. Moreover, an excess of anionic species is noted, which may be explained by the presence of moisture. Consequently, only the evolution of elemental analysis will be considered and not the absolute values, since the presence of water probably leads to overestimated oxygen value and underestimated nitrogen and boron values.

The nitrogen weight percent increases with the reaction temperature between 155 °C and 1000 °C (Fig. 1), while the oxygen weight percent decreases. The boron weight percent shows a little increase with the temperature process. Consequently, oxygen could be replaced by nitrogen in the boron oxide network.

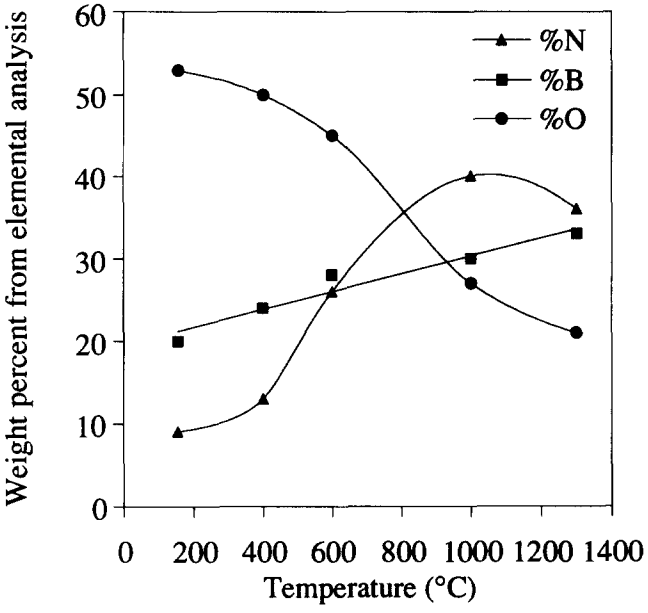

Fig. 1. Variation of nitrogen, oxygen and boron weight percent from elemental analysis versus nitridation temperature.

Table 1
Weight percent of nitrogen, oxygen and boron from elemental analysis, atomic ratio N/O and ceramic yields *Y*

Temperature (°C)	155	400	600	1000	1300
%N	9.1	13	26	40	36
%O	53	50	45	27	21
%B	20	24	28	30	33
N/O	0.19	0.29	0.66	1.69	1.96
Y	0.80	0.76	0.67	0.60	0.54

Boric acid reacts with ammonia at very low temperature and the N/B ratio increases from 0.3 at 155 °C to 0.7 at 600 °C and almost 1 at 1000 °C. The slight decrease observed at 1300 °C may be due to the formation of molten boric oxide during pyrolysis which may inhibit the nitridation.

Nitridation is a reaction which occurs typically at a temperature of 600 °C, when ammonia is dissociated into N_2 and H_2. Boric acid seems to react even without the decomposition reaction of ammonia. A reaction of partial -OH substitution by $-NH_2$ groups could explain the introduction of nitrogen below 600 °C:

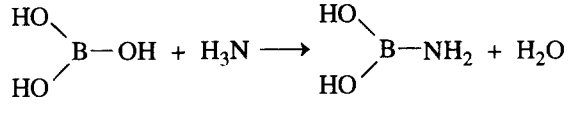

3.2. X-ray diffraction analysis

X-ray diffraction patterns are reported in Fig. 2. Boric acid is a crystalline compound which consists of sheets of $B(OH)_3$ molecules, linked together via hydrogen bonds, with a quasi hexagonal symmetry [21–22]. The

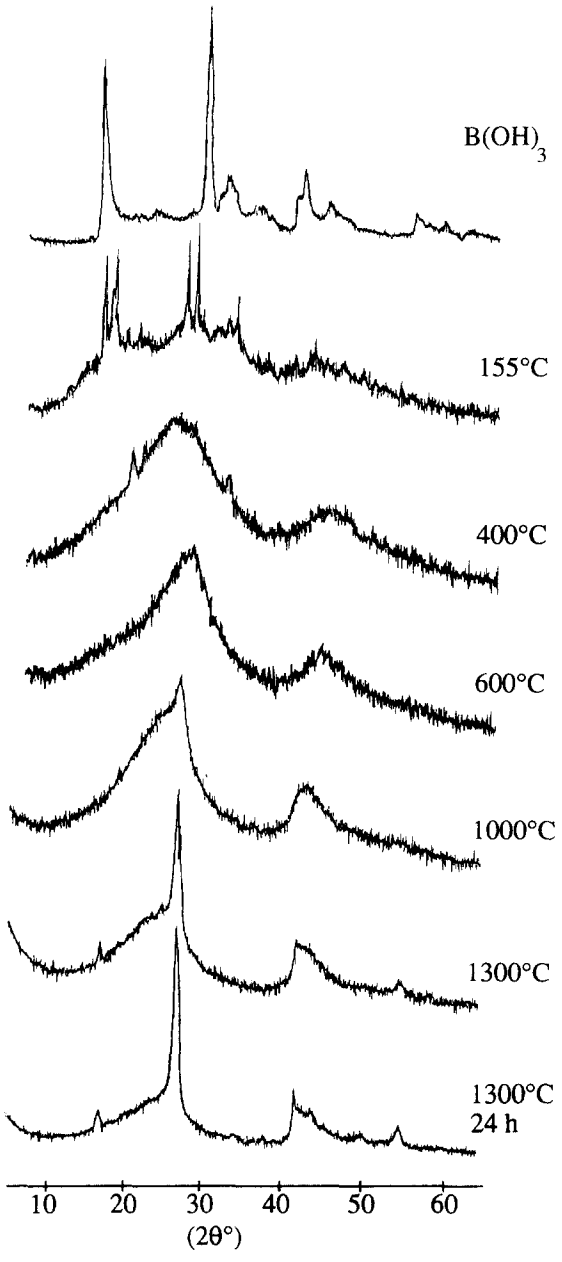

Fig. 2. XRD spectra of nitrided samples.

spectrum of the 155 °C nitrided sample consists of a partially crystallized unknown phase, probably involving amino species. This phase has been observed in the reaction between boric acid and urea [23]. The spectrum of the 400 °C sample is due to turbostratic boron nitride, with an interlayer distance d_{002} almost equal to 3.6 Å [2]. The spectrum of boric acid nitrided at 600 °C is almost the same, but the interlayer distance has decreased to 3.4 Å. The spectrum of the 1000 °C sample seems to be due to two phases of turbostratic boron nitride, a very disordered one, with $d_{002}=3.5$ Å and a more organized one with $d_{002}=3.3$ Å. This latter interlayer distance is the same as in the hexagonal boron nitride form. The spectrum of the 1300 °C nitrided sample is due to turbostratic boron nitride ($d_{002}=3.33$) since 100 and 101 lines are not resolved and the 102 line is not observed [19]. Trace quantities of boric oxide are also observed.

3.3. Infrared analysis

The low frequency infrared spectra of nitrided samples are represented in Fig. 3. Boric acid exhibits bands at 1450, 1180 and 760 cm^{-1} attributed to ν(BO), δ(BOH) and δ(BOB), respectively, and two narrow bands at 650 and 545 cm^{-1} attributed to $\delta(BO_3)$ and δ(OBO), respectively [22]. The spectrum of the 155 °C sample is very different. Some boric acid bands have disappeared and new bands are present at 1400 and 1340 cm^{-1} (ν(B–O)), 1230, 1080, 1000, 900, 750 and 665 cm^{-1}. The bands at 1080, 1000 and 900 cm^{-1} could be due to tetrahedral boron units [24]. The shift of the ν(B–O)

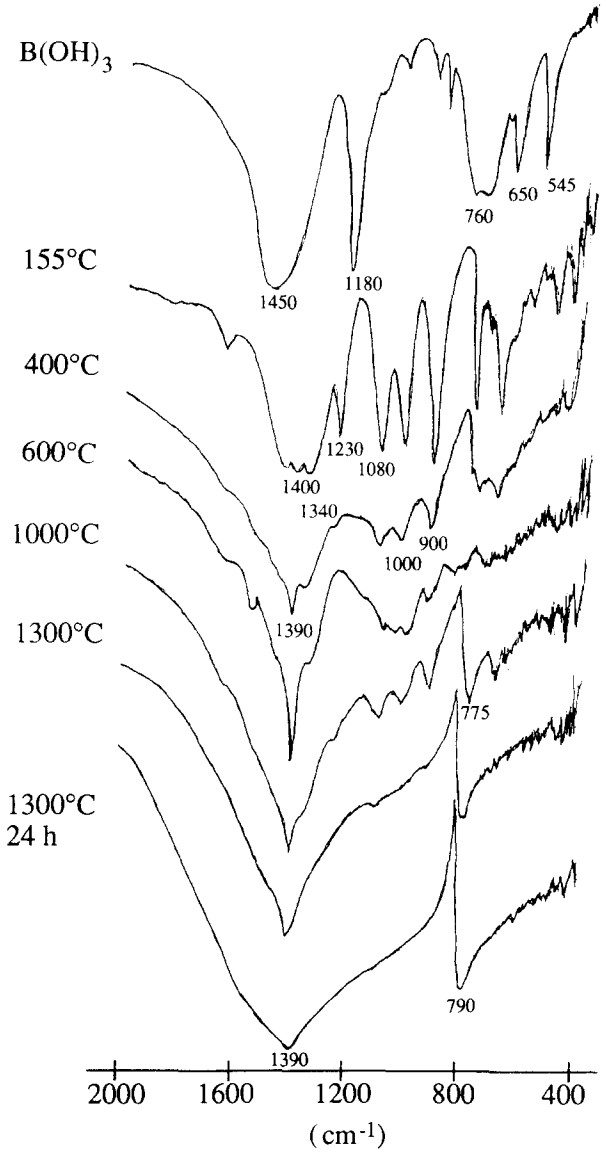

Fig. 3. Low-frequency infrared spectra of nitrided samples.

vibration is explained by a dehydratation reaction of boric acid to metaboric acid HBO_2 [22].

The 400 °C and the 600 °C sample infrared spectra present a narrow band at 1390 cm^{-1} which is attributed to the stretching ν(BN) vibration [5]. The lower frequency bands at 1080, 1000 and 900 cm^{-1} are less intense. They may be attributed to boron oxynitride species [23]. The spectrum of the 1000 °C sample consists of bands around 1400 cm^{-1} with a maximum at 1390 cm^{-1}. The other band of boron nitride at 775 cm^{-1} is observed [5]. At 1300 °C, the spectrum shows two bands due to boron nitride at 1390 cm^{-1} and 790 cm^{-1} [1,5,13].

The high frequency infrared spectra of nitrided samples are represented in Fig. 4. Boric acid exhibits a band at 3200 cm^{-1}, attributed to ν(OH). At 155 °C, two vibration bands at 3360 and 3450 cm^{-1} appeared and the 3250 cm^{-1} band shifted to 3140 cm^{-1}. The two first bands are due to NH_2 species [1,2], while the third one may be due to OH species. The intensity of the OH and NH bands reduces with temperature increase.

3.4. XPS analysis

The nitridation process has been followed by X-ray photoelectron spectroscopy. The B 1s, O 1s and N 1s binding energies of the nitrided samples are represented in Figs. 5 and 6 and in Table 2.

The 155 °C nitrided sample shows a symmetrical B 1s peak which could not be split into a doublet (Fig. 5). The corresponding binding energy of this line is 192.8 eV. For each sample treated at more elevated temperatures under ammonia (> 155 °C), it was possible

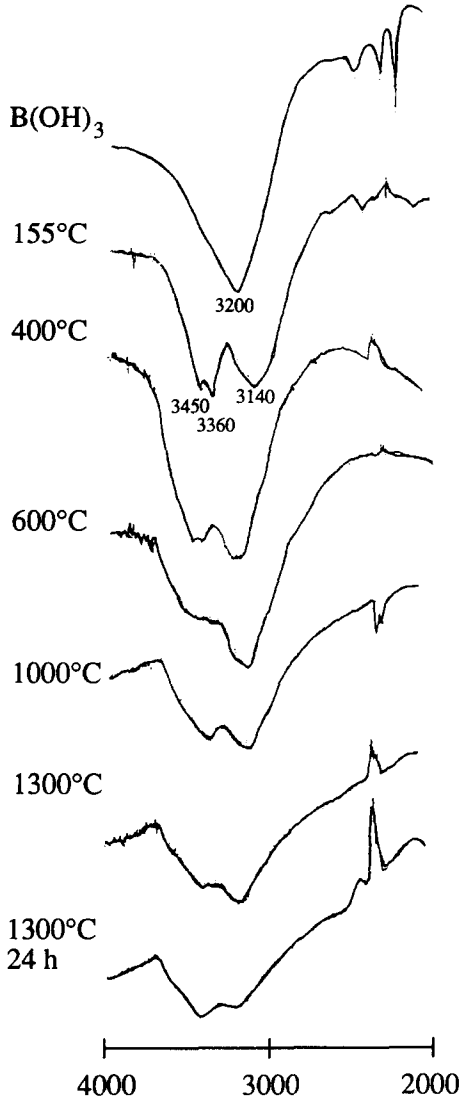

Fig. 4. High-frequency infrared spectra of nitrided samples.

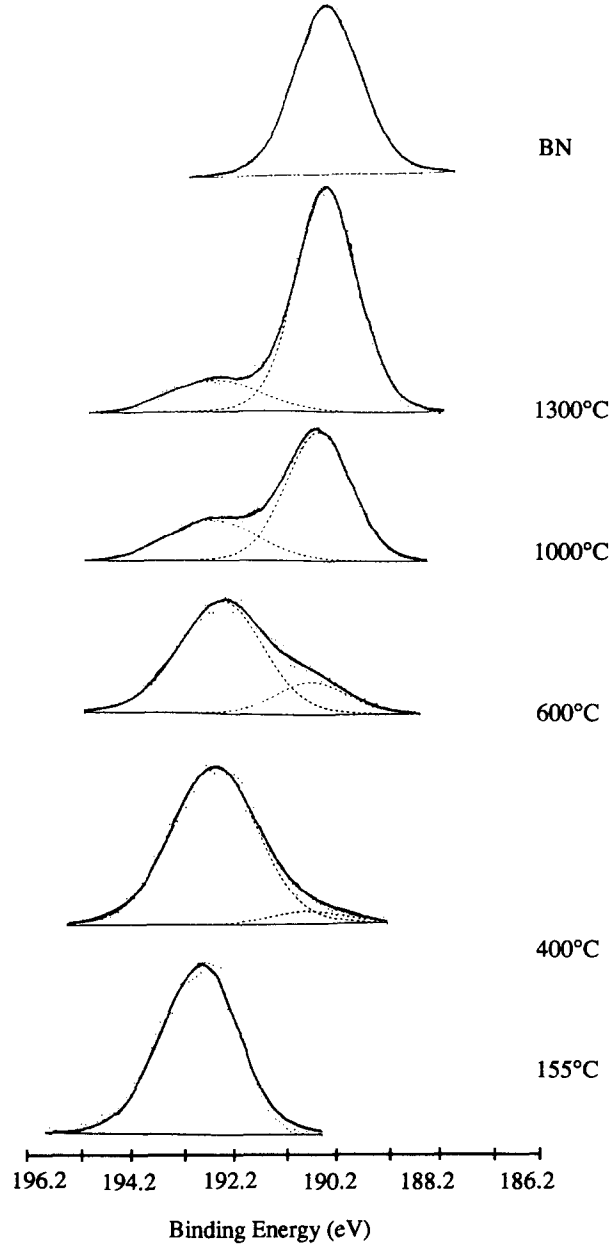

Fig. 5. B 1s spectra of nitrided samples.

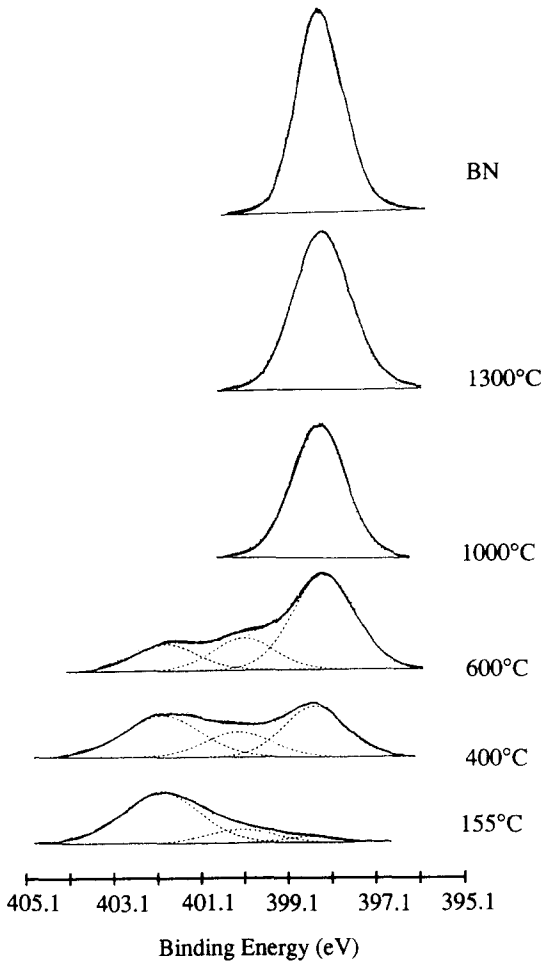

Fig. 6. N 1s spectra of nitrided samples.

Table 2
B 1s, O 1s and N 1s binding energies (eV) of boron oxynitride, boron nitride and boron oxide samples (FWMH in parenthesis (eV))

Temp (°C)	B 1s		O 1s	N 1s		
155	–	192.8	532.5	398.4	399.9	401.9
		(1.8)	(2.1)	(1.7)	(1.7)	(2.0)
400	190.8	192.6	532.4	398.4	400.2	401.9
	(1.7)	(2.0)	(2.2)	(1.7)	(1.7)	(1.9)
600	190.8	192.6	532.4	398.3	400.1	401.9
	(1.7)	(1.9)	(2.1)	(1.7)	(1.7)	(1.7)
1000	190.6	192.7	532.8	398.2	–	–
	(1.5)	(2.1)	(2.0)	(1.5)		
1300	190.5	192.7	532.7	398.4	–	–
	(1.4)	(2.1)	(2.1)	(1.4)		
BN	190.7	–	532.6	398.2	–	–
	(1.3)		(1.9)	(1.2)		
B_2O_3		193.7	532.5			
$B(OH)_3$		192.8				

to decompose the B 1s band into two components: a high energy one within the 192.7–192.8 eV range and a low energy one within the 190.5–190.8 eV range. Fig. 5 and Table 3 show the relative area evolution of the two B 1s components at increasing temperatures. The

Table 3
Relative area of the B 1s and N 1s components

Temp (°C)	B 1s		N 1s		
	BN_x	BO_x	$N_{network}$	$-NH_2$, $>NH$	$-NH_3^+$
155	0	100	6	19	75
400	5	95	42	22	36
600	20	80	62	19	19
1000	72	28	100	0	0
1300	83	17	100	0	0
BN	100	0	100	0	0

intensity of the low energy component increases while the high energy component decreases from 400 °C to 1300 °C.

The low energy signal, within the 190.5–190.8 eV range, is assigned to an atomic arrangement surrounding the boron atom consisting of only nitrogen atoms, similar to that occurring in pure hexagonal boron nitride (190.7 ± 0.2 eV).

The high energy component (192.8 eV) corresponds to an intermediate state between pure B_2O_3 oxide (B 1s = 193.7 eV) [7] and pure hexagonal BN nitride (B 1s = 190.7 eV) [6,7,9,25]. Thus, it could be assigned to a boron atom in a mixed oxygen–nitrogen surrounding. Therefore, the value of the B 1s binding energy agrees with the replacement of an oxygen atom bonded to a boron atom by a less electronegative nitrogen atom, which causes a decrease in the binding energies of the boron core electrons. This result is in agreement with the works of C. Guimon et al. [7,8]. They attributed a B 1s peak at 192.2 eV to the occurrence of BO_xN_y species in their BN films. Recently, it has been noted [6] that two binding energies are observed at 191.8 eV and 192.6 eV on BN films, which could be due to BN_2O units and to BNO_2 units, respectively. However, it must be noted that the B 1s binding energy of boric acid is also reported at 192.8 eV [26], which means that boron linked to terminal species will be observed within the same range as boron oxide substituted by nitrogen.

Therefore, from these results, the reaction of ammonia with boric acid leads to a mixture of two phases: a pure boron nitride (B 1s = 190.7 eV, denoted BN_x) and a boron oxide phase more or less nitrided (B 1s = 192.8 eV, denoted BO_x) [16]. The boron nitride phase component increases with increasing temperature treatment.

The O 1s binding energies with the 532.4–532.8 eV range agree with reported values of 532.6 eV for CVD BN films [7].

The N 1s spectra of the boron oxynitride samples prepared at 155, 400 and 600 °C are composed of overlapping peaks indicative of nitrogen present in more than one chemical form (Fig. 6). We choose to separate this N 1s spectra into three components which were

assigned to $N_{network}$ species (398.3±0.2 eV) [7,9,23,25], $-NH_2$ or >NH species (400.0±0.2 eV) [23] and $-NH_3^+$ species (401.9±0.2 eV) (Table 3). The N 1s binding energy of the $N_{network}$ species agree with the observed value of 398.2±0.2 eV for commercial BN powder and with reported values of 398.2 eV for chemical vapor deposited BN. The others forms of nitrogen show that ammonia strongly chemisorbs on the boric acid surface at relatively low temperature and are the predominant species of nitrogen (94%) for the 155 °C prepared sample. Increasing the temperature provokes a decrease in the adsorbed nitrogen and an increase in the nitrogen network amount (Table 3). Thus, for the 1000 °C prepared sample, only the $N_{network}$ line is observed.

The evolution of atomic percent of nitrogen, boron and oxygen in the pyrolyzed samples has been reported in Table 4 and Fig. 7. There is a great agreement between the intensity of the BN_x component and the intensity of the $N_{network}$ component. Moreover, the intensity of the BO_x component and the intensity of the oxygen signal are almost parallel. If the intensities are related to the different valencies, then there is

Table 4
Atomic percent of nitrogen, oxygen and boron from XPS analysis

Temp (°C)	B 1s		O 1s	N 1s		
	BN_x	BO_x		N_{net}	NH_2	NH_3^+
155	0	33.8	59.5	0.4	1.2	5.0
400	1.8	33.9	53.9	4.3	2.2	3.6
600	7.0	28.0	50.0	9.2	2.8	2.8
1000	30.7	11.9	24.6	32.6	0	0
1300	37.0	7.6	17.5	37.9	0	0

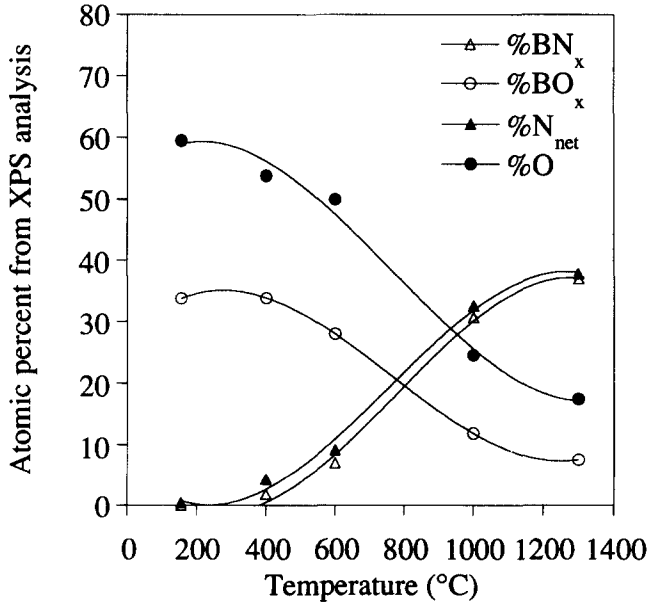

Fig. 7. Variation of nitrogen, oxygen and boron atomic percent from XPS analysis versus nitridation temperature.

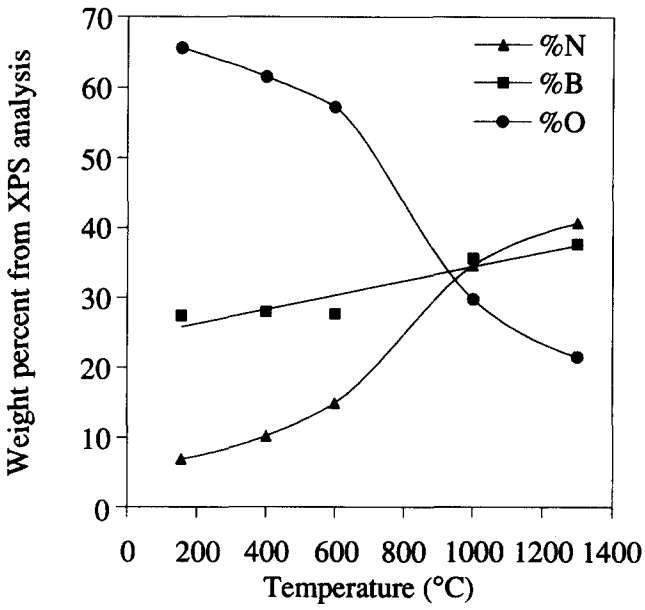

Fig. 8. Variation of oxygen, nitrogen and boron weight percent from XPS data versus temperature.

Table 5
Weight percent of nitrogen, oxygen, boron and atomic ratio N/O from XPS analysis

Temp (°C)	155	400	600	1000	1300	BN
%N	6.9	10.2	14.9	34.6	40.7	53.9
%O	65.6	61.6	57.3	29.8	21.5	4.1
%B	27.4	28.0	27.7	35.6	37.7	41.8
N/O	0.11	0.18	0.29	1.33	2.17	

good agreement concerning nitrogen sites, which means that 3*I (BN_x) is similar to 3*I ($N_{network}$).

Concerning oxygen sites, 2*I (O) is found to be a little greater than 3*I (BO_x), but their evolution seems to be linked. This could be explained by the occurrence of two boron sites, one of purely nitride and the other of oxide partially nitrided.

The evolution of the nitrogen, boron and oxygen weight percent from XPS analysis versus temperature are represented in Fig. 8 and Table 5. A similar evolution is observed between elemental analysis (Fig. 1) and XPS results (Fig. 8). Nevertheless, there is more boron and oxygen and less nitrogen from XPS data than from elemental analysis data.

4. Conclusions

When boric acid is heated under flowing ammonia, two stages are observed. Boric acid reacts with ammonia at very low temperature (155 °C) in an -OH by $-NH_2$ substitution and probably by a NH_3 addition process, as suggested by the N 1s binding energies due to NH_3^+ and NH_2 species and by the NH_2 vibration band observed

by infrared spectroscopy. An unknown crystalline compound is then formed. From 400 °C to 1300 °C, the nitridation reaction leads to the formation of a turbostratic boron nitride phase. B–N bonds are clearly observed by IR at 400 °C. XPS analysis suggests the occurrence of only two boron environments: some boron nitride sites and some boron mostly surrounded by oxygen sites whose intensity decreases from 400 °C to 1300 °C. A beginning in the organization of turbostratic boron nitride is observed at 1300 °C. The 1300 °C pyrolyzed sample consists of turbostratic boron nitride and some amorphous boron oxide or oxynitride units.

Acknowledgments

We would like to thank the "Service Central d'Analyse du CNRS" for elemental analysis.

References

[1] R.T. Paine and C.K. Narula, *Chem. Rev., 90* (1990) 73.
[2] M.I. Baraton, T. Merle, P. Quintard and V. Lorenzelli, *Langmuir, 9* (1993) 1486.
[3] D. Seyferth and W.S. Rees Jr., *Mat. Res. Soc. Symp. Proc., 121* (1988) 449.
[4] D. Fister, *Ceram. Eng. Sci. Proc., 6* (1985) 1305.
[5] A.S. Rozenberg, Y.A. Sinenko and N.V. Chukanov, *J. Mat. Sci., 28* (1993) 5675.
[6] V. Cholet, L. Vandenbulcke, J.P. Rouan, P. Baillif and R. Erre, *J. Mat. Sci., 29* (1994) 1417.
[7] C. Guimon, D. Gonbeau, G. Pfister-Guillozo, O. Dugne, A. Guette, R. Naslain and M. Lahaye, *Surf. Int. Anal., 16* (1990) 440.
[8] O. Dugne, A. Prouhet, R. Guette, R. Naslain, K. Fourmeaux, J. Sevely, C. Guimon, D. Gonbeau and G. Pfister-Guillouzo, *J. Phys., C5, 50* (1989) 333.
[9] G.M. Ingo, *Thin Solids Films, 228* (1993) 276.
[10] L. Maya, *Mat. Res. Soc. Symp. Proc., 121* (1988) 455.
[11] R.R. Rye and D.R. Taillant, *Chem. Mater., 3* (1991) 286.
[12] S.I. Hirano, A. Fujii, T. Yogo and S. Naka, *J. Am. Ceram. Soc., 73* (8) (1990) 2238.
[13] C.K. Narula, R.T. Paine and R. Schaeffer, *Mat. Res. Soc. Symp. Proc., 73* (1986) 383.
[14] D. Seyferth and W.S. Rees, Jr., *Chem. Mater., 3* (1991) 1106.
[15] K.J.L. Paciorek, S.R. Masuda, R.H. Kratzer and W.R. Schmidt, *Chem. Mater., 3* (1991) 88.
[16] V. Brozek, M. Hubacek, *J. Sol. State. Chem., 100* (1992) 120.
[17] Z. Gontarz and S. Podsiadlo, *Pol. J. Chem., 58* (1984) 3.
[18] A.E. Lindemanis, *Mater. Sci. Res., 17* (1984) 111.
[19] J.Y. Choi and S.J.L. Kang, *J. Am. Ceram. Soc., 76* (10) (1993) 2525.
[20] J.H. Scofield, *J. Electron. Spectr. Relat. Phenom., 8* (1976) 129.
[21] W.H. Zachariasen, *Acta Crystallogr., 7* (1954) 305.
[22] J.L. Parsons and M.E. Milberg, *J. Am. Ceram. Soc., 43* (6) (1960) 326.
[23] M. Hubacek, T. Sato and T. Ishii, *J. Sol. State. Chem., 109* (1994) 384.
[24] E.I. Kamitsos, M.A. Karakassides and G.D. Chryssikos, *J. Phys. Chem., 91* (1987) 1073.
[25] T. Goto, T. Hirai, *J. Mat. Sci. Lett., 7* (1988) 548.
[26] D.J. Joyner and D.M. Hercules, *J. Chem. Phys., 73* (2) (1980) 1095.